ADVANCED HEALTHCARE MATERIALS

Supporting Information

for *Adv. Healthcare Mater.,* DOI: 10.1002/adhm.202000918

Precision 3D-Printed Cell Scaffolds Mimicking Native Tissue Composition and Mechanics

Amelie Erben, Marcel Hörning, Bastian Hartmann, Tanja Becke, Stephan A. Eisler, Alexander Southan, Séverine Cranz, Oliver Hayden, Nikolaus Kneidinger, Melanie Königshoff, Michael Lindner, Günter E.M. Tovar, Gerald Burgstaller, Hauke Clausen-Schaumann, Stefanie Sudhop, Michael Heymann**

Supporting Information

Precision 3D-Printed Cell Scaffolds Mimicking Native Tissue Composition and Mechanics

Amelie Erben, Marcel Hörning, Bastian Hartmann, Tanja Becke, Stephan A. Eisler, Alexander Southan, Séverine Cranz, Oliver Hayden, Nikolaus Kneidinger, Melanie Königshoff, Michael Lindner, Günter E.M. Tovar, Gerald Burgstaller, Hauke Clausen-Schaumann, Stefanie Sudhop, Michael Heymann**

This PDF file includes:

1. Movies:
   - Movie S1: Time lapse of hMSCs on scaffold.
   - Movie S2: Time lapse of primary human lung fibroblasts (phLFs) on scaffolds.
   - Movie S3: Confocal zStack movie of stained hMSCs on scaffold.
   - Movie S4: 3D rendered volume of printed alveoli geometry with phLFs.
2. Tables:
   - Table S1: Literature on protein-based TPS printing.
   - Table S2: Printing times.
   - Table S3: CAD designs.
   - Table S4: Detailed Sample Data regarding AFM measurements.
3. Figures:
   - Figure S1: Fluorescence images of phLFs on high-precision 3D printed scaffolds.
   - Figure S2: Process parameters for GM10-LAP.
   - Figure S3: Shading correction of image tiles.
4. References

***Movie S1*:** Time lapse movie of hMSCs cultured on BSA high-precision 3D printed scaffolds for 60 hours (Figure 2).

***Movie S2*:** Time lapse movie of primary human lung fibroblasts (phLFs) cultured on GM10 – RB (top left and middle) and coated with fibronectin (top right), GelMa-RB (bottom left and middle) and BSA&GelMA-RB high-precision 3D printed scaffolds (Figure 2).

***Movie S3*:** Confocal z-stack of hMSCs on BSA-RB mesh-like high-precision 3D printed scaffolds (Figure 2).

***Movie S4*:** 3D rendering of a confocal stack of TPS printed alveoli geometry with GM10 and LAP (grey) and colonized with with phLFs for 96 hours (phalloidin staining, red, Figure 6).

***Table S1*:** Literature on scaffolds printed with TPS and protein-based resins for cellular applications. Scaffolds printed with bovine serum albumin (BSA) and rose bengal (RB) are marked in pink, scaffolds printed with a gelatin methacryloyl derivative and lithium-(2,4,6-trimethylbenzoyl)-phenylphosphinate (LAP) in grey. Individual resin recipes are separated by a comma, whereas individual components of one resin recipe are separated by '&'.

photo-polymer	**photo-initiator**	**scaffold geometry**	**cell type**	**cellular response**	**ref.**
type I, II, IV collagen, BSA	RB, benzophenone dimer	lines	dermal fibroblasts	cell adhesion	Basu et al. 2005[1]
BSA (& laminin)	RB	arches	H9 embryonic stem cell derived human mesenchymal stem cells (MSCs)	cell interaction	Su et al. 2012[2]
BSA, avidin, lysozyme	Eosin Y, methylene blue (MB)	unconstrained 3D structures	none		Spivey et al. 2013[3]
BSA	RB	pillars	mouse 3T3 fibroblasts (ATCC)	3D morphology	Chan et al. 2014[4]
BSA	RB	crosses	none		Lay et al. 2016[5]
BSA, fibronectin	RB	pillars	human mesenchymal stem cells	maturation of fibrillar adhesion	Ma et al. 2017[6]
BSA	RB	ring	mouse fibroblasts (L929)	modulation of single cell behavior	Nishiguchi et al. 2020[7]
BSA, collagen type-IV, avidin, IP-L	flavin adenine dinucleotide (FAD), rhodamine B	icosahedral unit and patterns embedded in photoresist backbone	NIH/3T3 cells, Rat adrenal pheochromocytoma PC12 cells	adhesion, migration and interaction	Serien and Takeuchi 2017[8]
collagen type I, gelatin, hyaluronic acid	MB	perforated 3D disc	human iPSCs, rat retinal cells	cell viability	Shrestha et al. 2019[9]
GelMOD	Irgacure 2959	woodpiles	human adipose-derived stem cells (ASCs)	adhesion, proliferation, differentation	Ovsianikov et al. 2010[10]
gelatin methacrylamide (Gel-MAAm)	Irgacure 2959	lines	primary chondrocytes	adhesion and orientation	Engelhardt et al. 2011[11]
GelMa & PEGDA	P2CK (benzylidene cycloketone-based)	woodpiles	human BJ (hBJ) foreskin fibroblasts	adhesion, viability and structural invasion	Brigo et al. 2017[12]
gel-MOD-AEMA	P2CK	logo	mouse fibroblast cells (L929), mouse calvaria-derived preosteoblast cells (MC3T3-E1)	metabolic activity	Van Hoorick et al. 2017[13]
acrylamide-modified gelatin	azo-crosslinker & Irgacure 369	hollow cylinders	human dermal fibroblasts (neonatal HDF 106-05n ECACC)	alignment and orientation	Pennacchio et al. 2018[14]

GelMOD-AEMA	lithium-(2,4,6-trimethylbenzoyl)-phenylphosphinate (LAP)	hydrogel membrane	human umbilical-vein endothelial cells (HUVEC) and human choriocarcinoma cells (BeWo B30)	cell-layer formation	Mandt et al. 2018[15]
GelMA, Chitosan	eosin Y	woodpiles	human dental pulp stem cells (DPSCs)	adhesion and proliferation	Parkatzidis et al. 2019[16]
silk fibroin	MB	microwire and microdot arrays	mouse fibroblast cell line, L929	biocompa-tibility	Sun et al. 2015[17]
silk fibroin	none	y-shape	human mesenchymal stem cells (hMSCs), human foreskin fibroblasts	n.a.	Applegate et al. 2015[18]
chitosan-g-Oligolactide, PEGDA	Irgacure 2959	pillars	none	n.a.	Demina et al. 2017[19]
BSA (& GelMa)	RB	alveolar scaffolds, patterned substrates with (sub-) cellular resolution, mesh on posts	human mesenchymal stem cells (hMSCs), mouse tendon stem/progenitor cells (mTSPCs), murine NIH3T3 fibroblast wildtype cells (NIH3T3 WT), human umbilical vein endothelial cells (HUVECs), primary human lung fibroblasts (phLFs), mouse myoblast cells (C2C12)	good adhesion with fibronectin coating	this study
GM10	LAP, RB			good adhesion enhanced by fibronectin coating, cellular actin alignment within constrained topographies	

***Table S2*:** Theoretical printing times of alveolar print template for print volumes of 0.00513 mm^3 and 1 mm^3 with laser scan speeds of 35 mm s^{-1} and 70 mm s^{-1} calculated by Describe slicer software (Nanoscribe GmbH) with 0.3 µm z-slicing and 0.2 µm x/y-hatching for a 63x objective or 1 µm z-slicing and 0.5 µm x/y-hatching for a 25x objective. For the solid settings, the structure's interior is fully, whereas for shell settings it is only partially printed. In this example, the parameters for shell settings were chosen to fully print the alveolar wall structure (Figure 1A). However, time differences arise in comparison to solid settings due to a modified laser path.

volume [mm^3]	**scan speed [mm s^{-1}]**	**63x - solid**	**25x - solid**	**25x - shell**
0.00513	35	1:47:00 h	0:06:31 h	0:06:02 h
0.00513	70	2:14:00 h	0:06:01 h	0:05:14 h
1.0	35	347:45 h	21:11 h	19:36 h
1.0	70	435:30 h	19:33 h	17:00 h

***Table S3*:** CAD designs of high-precision 3D printed scaffolds. The respective STL-files are provided.

	design D1		design D4
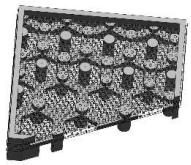	design D2 D2-frame D2-top mesh (5 µm) D2-bottom mesh (2.5 µm)	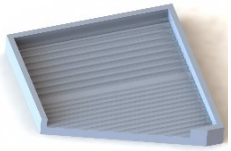	design D5
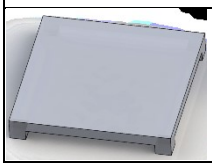	design D3		design D6

Table S4: *Detailed sample data regarding AFM measurements including the number of individual samples, the number of individual measurements and the evaluated indentation depth.*

diagram name	**samples**	**measurements**	**indentation depth [µm]**
number of indentations	1	100 / 400 / 1600	0 - 2
positions	2	98 / 99 / 372 / 97	0 - 2
cell culture conditions	1	503 / 510	0 - 1
PBS	1	503 / 512 / 509	0 - 1
scan speed & laser power	1	256	0 - 1
number of laser passes	1	384 / 267	top: 0 - 1; bulk: 1 - 2
objective magnification	1	236 / 155	0 - 1
BSA - GelMa & RB	1	500 – 1000 / time point	0 - 1
BSA & RB	1	385 / 493	top: 0 - 1; bulk: 1 - 2
GM10 & LAP	1	798 / 710	top: 0 - 1; bulk: 1 - 2

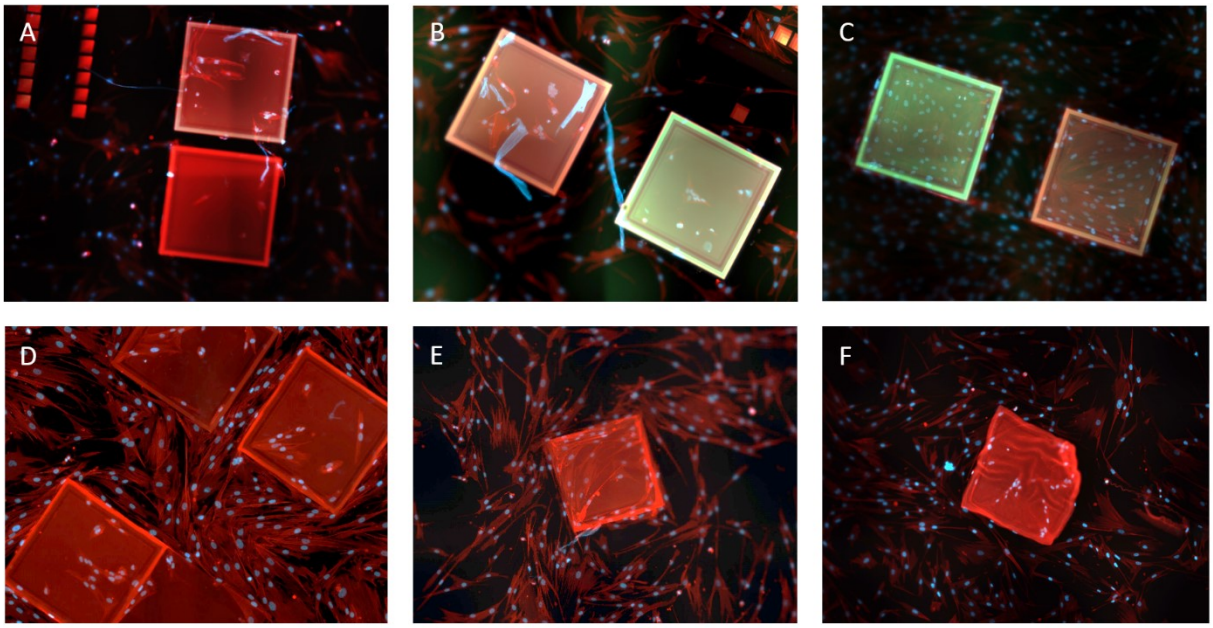

***Figure S1*:** phLFs stained with phalloidin for the actin cytoskeleton (red) and with DAPI for the cell nuclei (blue) cultivated on GM10 – RB (top, left and middle) and coated with fibronectin (top right), GelMa-RB (bottom left and middle) and BSA&GelMA-RB high-precision 3D scaffolds. Images were taken after 48 h of cell colonization.

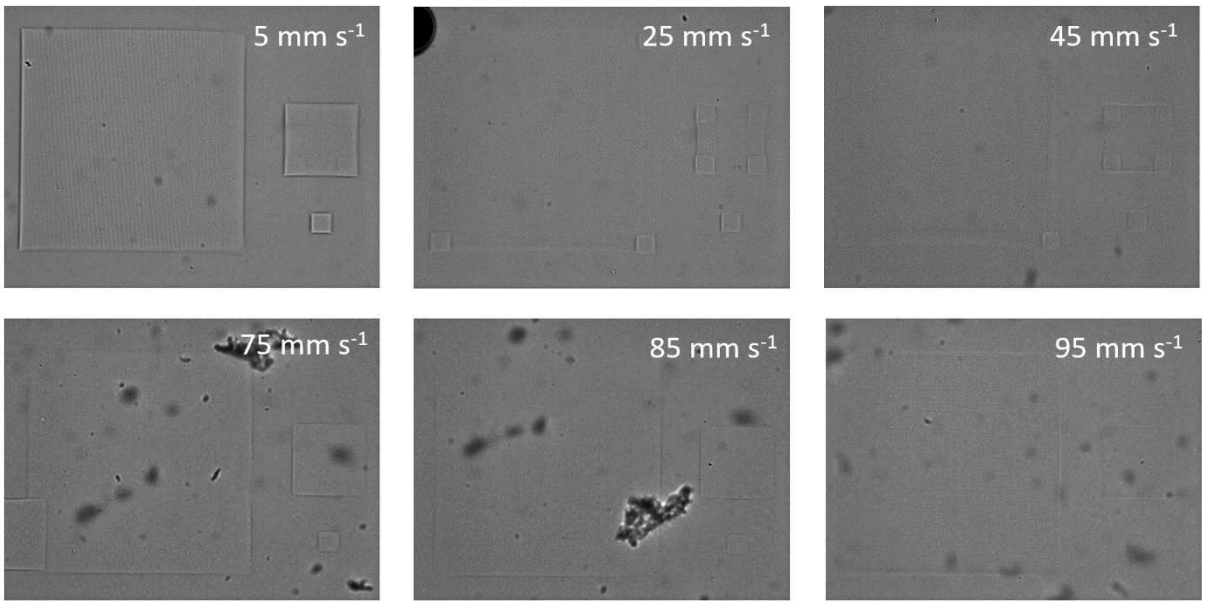

***Figure S2*:** Printing results for GM10-LAP resin compositions printed with 60 mW laser power and scan speeds ranging from 5 – 95 mm s^{-1}.

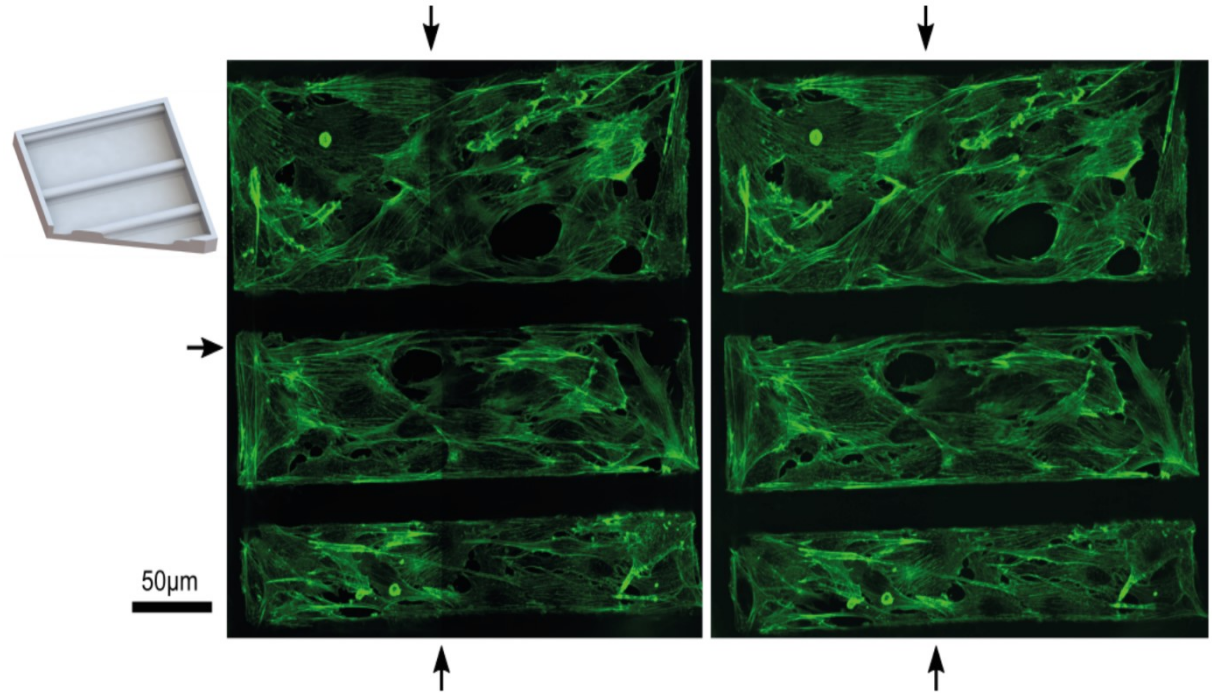

***Figure S3*:** Shading correction of image tiles. The ImageJ Plugin BaSiC[20] was applied prior to stitching in order to correct illumination shadings. Shown is an example before (left) and after (right) correction. Arrows indicate the stitch-interfaces of the four tiles that were stitched.

References:

[1] S. Basu, L. P. Cunningham, G. D. Pins, K. A. Bush, R. Taboada, A. R. Howell, J. Wang, P. J. Campagnola, *Biomacromolecules* **2005**, *6*, 1465.

[2] P. J. Su, Q. A. Tran, J. J. Fong, K. W. Eliceiri, B. M. Ogle, P. J. Campagnola, *Biomacromolecules* **2012**, *13*, 2917.

[3] E. C. Spivey, E. T. Ritschdorff, J. L. Connell, C. A. McLennon, C. E. Schmidt, J. B. Shear, *Adv. Funct. Mater.* **2013**, *23*, 333.

[4] B. P. Chan, J. N. Ma, J. Y. Xu, C. W. Li, J. P. Cheng, S. H. Cheng, *Adv. Funct. Mater.* **2014**, *24*, 277.

[5] C. L. Lay, Y. H. Lee, M. R. Lee, Y. Phang, X. Y. Ling, *ACS Appl. Mater. Interfaces* **2016**, *8*, 8145.

[6] J. Ma, C. Li, N. Huang, X. Wang, M. Tong, A. H. W. Ngan, B. P. Chan, *ACS Appl. Mater. Interfaces* **2017**, *9*, 29469.

[7] A. Nishiguchi, G. Kapiti, J. R. Höhner, S. Singh, M. Moeller, *ACS Appl. Bio Mater.* **2020**, *3*, 2378.

[8] D. Serien, S. Takeuchi, *ACS Biomater. Sci. Eng.* **2017**, *3*, 487.

[9] A. Shrestha, B. N. Allen, L. A. Wiley, B. A. Tucker, K. S. Worthington, *J. Ocul. Pharmacol. Ther.* **2019**, *00*, 1.

[10] A. Ovsianikov, A. Deiwick, S. Van Vlierberghe, M. Pflaum, M. Wilhelmi, P. Dubruel, B. Chichkov, *Materials (Basel).* **2010**, *4*, 288.

[11] S. Engelhardt, E. Hoch, K. Borchers, W. Meyer, H. Krüger, G. E. M. Tovar, A. Gillner, *Biofabrication* **2011**, *3*, DOI 10.1088/1758-5082/3/2/025003.

[12] L. Brigo, A. Urciuolo, S. Giulitti, G. Della Giustina, M. Tromayer, R. Liska, N. Elvassore, G. Brusatin, *Acta Biomater.* **2017**, *55*, 373.

[13] J. Van Hoorick, P. Gruber, M. Markovic, M. Tromayer, J. Van Erps, H. Thienpont, R. Liska, A. Ovsianikov, P. Dubruel, S. Van Vlierberghe, *Biomacromolecules* **2017**, *18*, 3260.

[14] F. A. Pennacchio, C. Casale, F. Urciuolo, G. Imparato, R. Vecchione, P. A. Netti, *Biomater. Sci.* **2018**, *6*, 2084.

[15] D. Mandt, P. Gruber, M. Markovic, M. Tromayer, M. Rothbauer, S. R. Adam Kratz, S. F. Ali, J. Van Hoorick, W. Holnthoner, S. Mühleder, et al., *Int. J. Bioprinting* **2018**, *4*, 1.

[16] K. Parkatzidis, M. Chatzinikolaidou, M. Kaliva, A. Bakopoulou, M. Farsari, M. Vamvakaki, *ACS Biomater. Sci. Eng.* **2019**, *5*, 6161.

[17] Y.-L. Sun, Q. Li, S.-M. Sun, J.-C. Huang, B.-Y. Zheng, Q.-D. Chen, Z.-Z. Shao, H.-B. Sun, *Nat. Commun.* **2015**, *6*, 8612.

[18] M. B. Applegate, J. Coburn, B. P. Partlow, J. E. Moreau, J. P. Mondia, B. Marelli, D. L. Kaplan, F. G. Omenetto, D. A. Weitz, *Proc. Natl. Acad. Sci. U. S. A.* **2015**, *112*, 12052.

[19] T. S. Demina, K. N. Bardakova, N. V. Minaev, E. A. Svidchenko, A. V. Istomin, G. P. Goncharuk, L. V. Vladimirov, A. V. Grachev, A. N. Zelenetskii, P. S. Timashev, et al., *Polymers (Basel).* **2017**, *9*, DOI 10.3390/polym9070302.

[20] T. Peng, K. Thorn, T. Schroeder, L. Wang, F. J. Theis, C. Marr, N. Navab, *Nat. Commun.* **2017**, *8*, 1.